Fermi Surface of Indium from Magnetoacoustic Measurements

J. A. RAYNE AND B. S. CHANDRASEKHAR
Westinghouse Research Laboratories, Pittsburgh, Pennsylvania
(Received November 1, 1961)

Magnetoacoustic measurements have been made at 91 Mc/sec on single-crystal specimens of indium. From the observed oscillatory behavior, the dimensions of the Fermi surface of indium have been obtained. The second-zone surface agrees very well with that predicted from the nearly free electron model, apart from a general reduction of about ten percent in all dimensions. Poorer agreement is found for the third-zone surface. The high-field attenuation for each propagation direction studied reached a saturation value, indicating an absence of open orbits in these directions.

I. INTRODUCTION

INDIUM is trivalent and is face-centered tetragonal, the c/a ratio at absolute zero being approx. 1.08. Thus it is very similar to aluminum, which is also trivalent and has a face-centered cubic structure. Extensive theoretical and experimental studies have shown that the band structure of the latter conforms very closely to that predicted by the "nearly free electron approximation".[1] It therefore would be of interest to determine whether this model was also applicable to the band structure of indium.

Comparatively little experimental data relating to the Fermi surface of indium has hitherto been available. De Haas-van Alphen data are insufficient to give any useful information about its band structure.[2] The recent magnetoacoustic measurements of Galkin *et al.*[3] do not give a very clear picture of the Fermi surface of indium owing to the scatter of their data and the fact that only two crystal orientations were studied in detail.

This paper describes independent magnetoacoustic measurements on ultra-pure zone-refined indium, in which the electron mean-free path was several millimeters as compared to the value of 0.3 mm in the material used by Galkin *et al.* Owing to the attendant increase in both the magnitude and number of oscillations, considerably greater precision was achieved in the determination of the extremal dimensions of the Fermi surface. This circumstance, together with the larger number of specimens studied, has resulted in a reasonably complete picture of the second zone Fermi surface for indium. Although the linear dimensions appear to be about 10% smaller than those predicted by the free-electron approximation, the general shape is quite close to that expected from this simple model. Rather fragmentary data for the third zone surface have been obtained, but the agreement with the predictions of the free-electron model appears to be much poorer in this case.

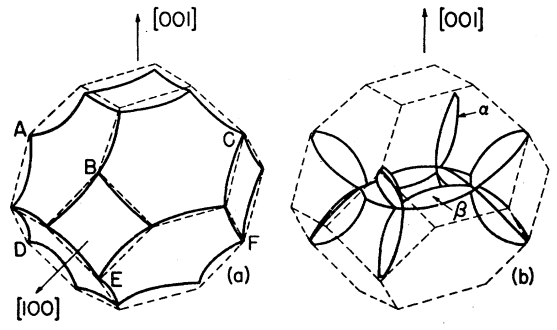

FIG. 1. Fermi surface of indium on free-electron approximation: (a) second-zone surface, (b) third-zone surface.

II. EXPERIMENTAL TECHNIQUE

The ultrasonic techniques used in this work were similar to those used by other workers.[4] Transmission measurements of attenuation were made at 91 Mc/sec using the two-crystal method, the transducers being excited at the third harmonic with 1-μsec electrical pulses generated by an Arenberg[5] transmitter. The receiver consisted of four cascaded chain amplifiers,[6] the rectified output of which was displayed on a Tektronix 545 oscillograph. A type-Z preamplifier allowed accurate measurement of the amplitude of the received pulse. At the frequency used in these experiments, the attenuation at low temperatures was so high that only one transmitted echo could be detected. The relative change in attenuation with applied field could thus only be obtained by measuring the attendant change in the amplitude of this pulse. Since the bond losses are presumably independent of field, however, no appreciable error was introduced by this procedure. All data were corrected for nonlinearity of the receiver.

The starting material for producing the single crystals used in this work was zone refined, special research-grade indium obtained from the Consolidated Mining and Smelting Company, Canada. The stated purity was in excess of 99.9999%. Cylindrical single crystals 2.5 cm in diameter and 10 cm in length were grown from this stock in a tapered graphite crucible by a modified Bridgman technique. The crystals were oriented by the

[1] Walter A. Harrison, Phys. Rev. **118**, 1182 (1961).
[2] See D. Shoenberg, *Progress in Low-Temperature Physics*, edited by C. J. Gorter (North-Holland Publishing Company, Amsterdam, 1957), Vol. 2, p. 258.
[3] A. A. Galkin, E. A. Kaner, and A. P. Korolyuk, J. Exptl. Theoret. Phys. (U.S.S.R.) **39**, 1517 (1960) [translation: Soviet Phys.—JETP **12**, 1055 (1961)].
[4] See for example, R. W. Morse, *Progress in Cryogenics* (Heywood and Company, Ltd., London, 1959), Vol. I.
[5] Arenberg Ultrasonic Laboratory Inc., Model PG-650-C.
[6] Hewlett-Packard, Model 460B.

back-reflection Laue method and suitable specimens cut from them using an electric-spark technique.[7] Subsequent x-ray examination showed the cut faces to be quite free of surface damage and the specimens were used in the attenuation experiments without further preparation. Four crystal orientations were used, the propagation vectors being parallel to the normals of the (100), (001), (110), and (111) planes, respectively. In all cases it was found that gylcerin gave a satisfactory acoustic bond between the transducer and the specimen. Previously measured elastic[8] data for indium were used to obtain the wavelength of sound for the various propagation directions.

III. THEORY

(a) Oscillatory Attenuation

The theory of the magnetoacoustic effect for a spherical energy surface has been treated in detail by Kjeldaas

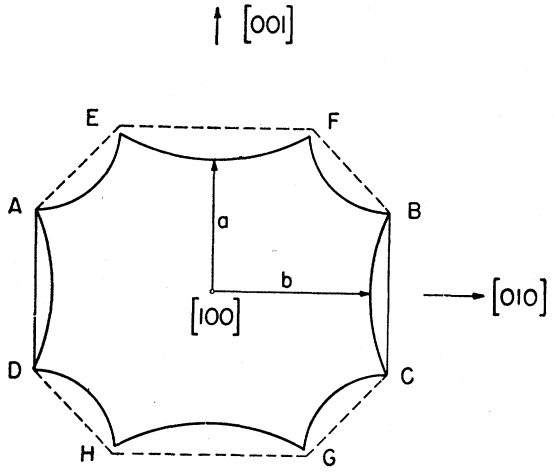

FIG. 2. Central section of second-zone surface perpendicular to [100].

and Holstein[9] and Cohen, Harrison and Harrison.[10] For more general types of Fermi surface, the effect has been studied by Gurevitch[11] and more recently by Pippard.[12] According to former, provided $ql \gg 1$, closed Fermi surfaces give rise to so-called harmonic oscillations in the attenuation. These oscillations are associated with electron orbits having an extremum in the direction of sound propagation and are given by an equation of the form

$$\alpha(H) \sim \alpha_0 \gamma^{-1}\{1+A(k\beta)^{-\frac{1}{2}} \sin(k\beta \pm \pi/4)\}. \quad (1)$$

In this expression α_0 is the zero-field attenuation, $\gamma = r/l$

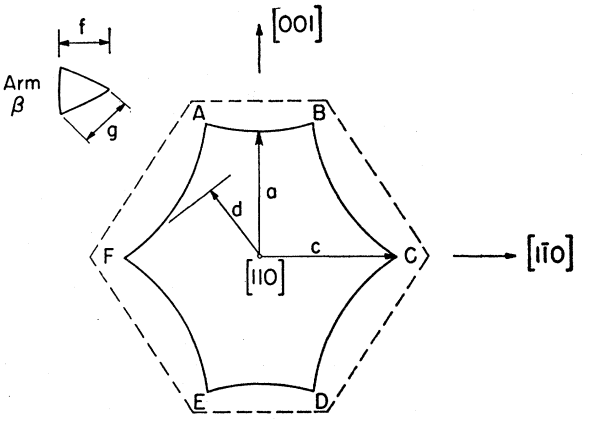

FIG. 3. Central sections of second- and third-zone surfaces perpendicular to [110].

where r is the orbit radius and l is the electron mean free path, $\beta = 2\pi\hbar c/\lambda eH$, k is the extremal diameter of the Fermi surface in the $[\mathbf{q}\times\mathbf{H}]$ direction of reciprocal space and $A \sim 1$. In the analysis due to Pippard, the oscillatory behavior is found to be the sum of contributions from all orbits depending on integrals of the form

$$I_n \approx A_n(\beta k)\eta_n^{(\text{ext})} \sin(\beta k + \delta_n). \quad (2)$$

Here A_n and δ_n are, respectively, amplitude and phase factors depending on the detailed orbit shape, and k is an *orbit* extremum in the $[\mathbf{q}\times\mathbf{H}]$ direction. It thus becomes impossible, when all orbits are considered, to determine which momentum dominates the oscillatory behavior for any given situation. In the following, however, we shall disregard such difficulties and assume with Gurevitch that the period of oscillation is essentially determined by the extremal dimension of the Fermi surface in the direction $[\mathbf{q}\times\mathbf{H}]$. From (1), the magnitude of this extremal *radius* is given by the

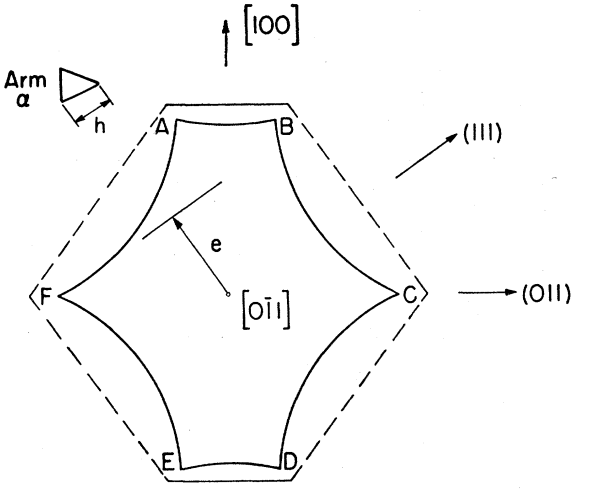

FIG. 4. Central sections of second- and third-zone surfaces perpendicular to [0$\bar{1}$1].

[7] B. S. Chandrasekhar, Rev. Sci. Instr. **32**, 368 (1961).
[8] B. S. Chandrasekhar and J. A. Rayne, Phys. Rev. **124**, 1011 (1961).
[9] T. Kjeldaas and T. Holstein, Phys. Rev. Letters **2**, 340 (1959).
[10] M. H. Cohen, M. J. Harrison, and W. A. Harrison, Phys. Rev. **117**, 937 (1960).
[11] V. L. Gurevitch, J. Exptl. Theoret. Phys. (U.S.S.R.) **37**, 71 (1959) [translation: Soviet Phys.—JETP **10**, 51 (1960)].
[12] A. B. Pippard, Proc. Roy. Soc. (London) **A257**, 165 (1960).

formula

$$k=\frac{e}{2\hbar c}\frac{\lambda}{\Delta(1/H)}, \tag{3}$$

λ being the sound wavelength.

For open orbits, there is also the possibility of so-called resonance oscillations.[3,13] In indium, however, the galvanomagnetic data[14] indicate that the Fermi surface is closed so that such oscillating behavior would not be present.

(b) Fermi Surface from Nearly Free Electron Model

From the data of Graham[15] *et al.* the axial ratio c/a of indium, extrapolated to absolute zero, is 1.08. There is thus a contraction of the Brillouin zone along the c axis in reciprocal space as shown in Fig. 1. Correspondingly, in the nearly free electron approximation, the faces of the Fermi surface in the second zone normal to the c axis are larger than those normal to the a axis.

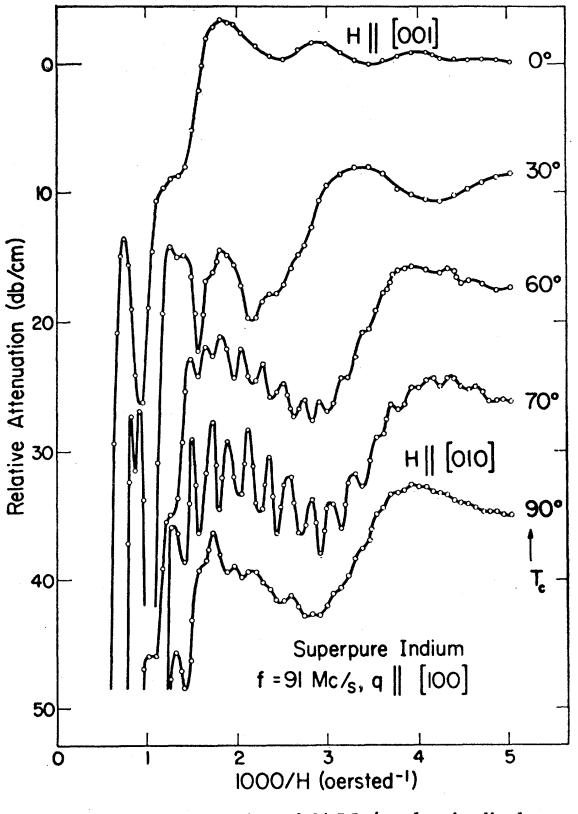

FIG. 5. Relative attenuation of 91-Mc/sec longitudinal waves propagating in [100] direction as a function of transverse magnetic field. The curves are displaced for clarity.

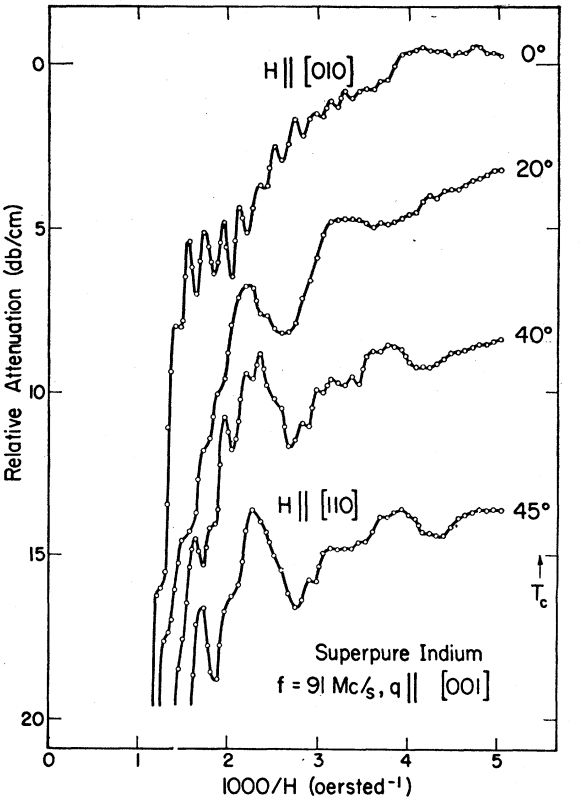

FIG. 6. Relative attenuation of 91-Mc/sec longitudinal waves propagating in [001] direction as a function of transverse magnetic field. The curves are displaced for clarity.

The free-electron sphere just passes through points such as *ABCDEF* on the latter type of face, so that on this model the second-zone surfaces would be multiply connected at these points. From the galvanomagnetic data of Alekseevskii and Gaidukov, however, there is no evidence of such multiple connection, since this would presumably give rise to open orbits, which are not observed experimentally. It must be concluded, therefore, that this feature of the model is not correct. In addition, the free-electron model also would predict small pockets of holes in the first and fourth zones. These presumably would be removed by the lattice potential. Unlike aluminum the arms α, β are no longer equivalent; although the connection between the arms is quite thin at some points, they apparently remain joined.

As in the case of aluminum, some modification of both the second and third zones would be expected in practice. In particular the sharp corners of intersection in the second zone presumably would become rounded, while the third-zone arms would have a modified shape. *A priori* one might expect much more drastic differences between the actual surface and that predicted from the free-electron model, since the conditions for the applicability of the latter are not well satisfied. Thus indium has a large ion core radius, violating the conditions for cancellation of the potential and kinetic energy terms

[13] E. A. Kaner, V. G. Peschanskii, and I. A. Privorotski, J. Exptl. Theoret. Phys. (U.S.S.R.) **40**, 214 (1961) [translation: Soviet Phys.—JETP **13**, 147 (1961)].
[14] N. E. Alekseevskii and Yu P. Gaidukov, JETP **37**, 672 (1959).
[15] J. Graham, A. Moore, and G. V. Raynor, J. Inst. Metals **84**, 86 (1955).

in the Hamiltonian, while its tetragonal structure indicates a $p_x p_y$ type of bonding which would remove the spherical symmetry of the wave function. It will be seen, however, that in spite of these apparent difficulties, the model does in fact give a very good approximation to the second-zone Fermi surface in indium. Central sections of the second and third zones obtained from the nearly free electron model are shown in Figs. 2 through 4.

IV. RESULTS AND DISCUSSIONS

(a) Magnetoacoustic Oscillations

The results of attenuation measurements for longitudinal waves at 91 Mc/sec with q both parallel and perpendicular to the applied field H, are given in Figs. 5 through 9. In all cases the temperature was approximately 2°K; this figure represents a compromise between the requirements of a long mean free path and the observability of low field oscillations free from effects due to the superconducting-to-normal transition. For the [100], [001], and [110] crystal orientations, data were obtained at 10-degree intervals in the direction of H with respect to a symmetry direction. Only representative curves have been plotted, however, because

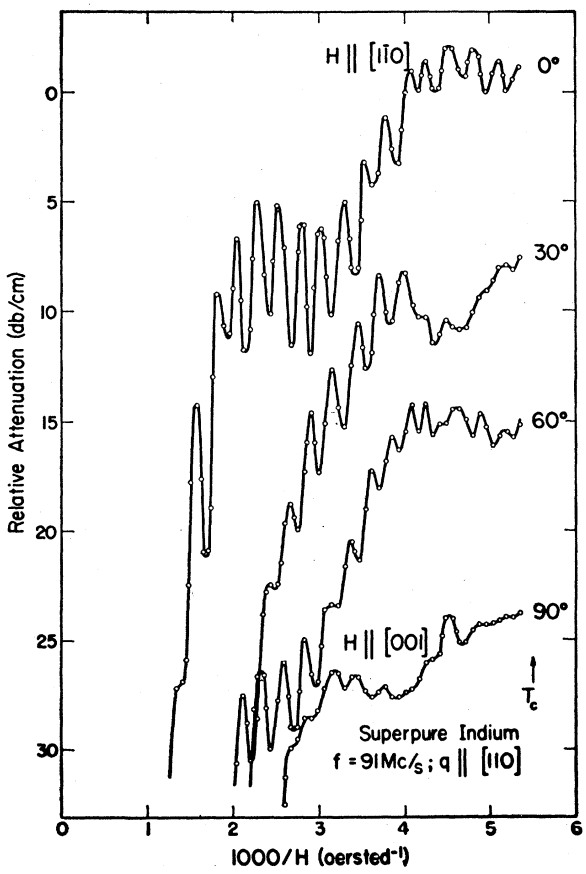

FIG. 7. Relative attenuation of 91-Mc/sec longitudinal waves propagating in [110] direction as a function of transverse magnetic field. The curves are displaced for clarity.

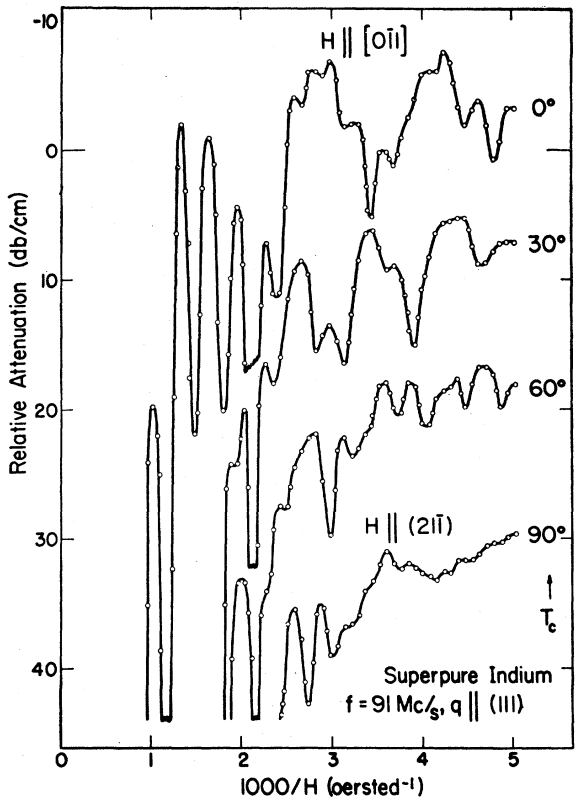

FIG. 8. Relative attenuation of 91-Mc/sec longitudinal waves propagating in (111) direction as a function of transverse magnetic field. The curves are displaced for clarity.

of space considerations. Attempts were also made to observe the attenuation of shear waves, but these were unsuccessful because of the very large zero-field attenuation of these modes.

It is noteworthy that, in many instances, at least 15 or more oscillations are observed. Now the electron mean free path is given by the relation

$$l=\pi(n+\tfrac{1}{2})\lambda, \tag{4}$$

where n is the order of the last oscillation clearly observable. Thus one obtains in this case $l\sim 2$ mm, which corresponds to a residual resistance ratio of about 50 000 to 1.

From Eq. (1), it follows that the attenuation maxima are periodic in $1/H$ and that a plot of the values of $1/H$ for these maxima versus the integers should be linear. Such a plot for $q\|[001]$ and $H\|[010]$ is shown in Fig. 10. It is believed that the presently available accuracy is insufficient to determine the phase factor [see Eqs. (1) and (2)], so that little significance should be attached to the fact that the straight line passes through the origin. Similar plots were used to determine the momenta corresponding to the various directions of **H** for each crystal orientation, the wavelengths λ in Eq. (3) being calculated from the low-temperature elastic data.[8] The resulting momenta are plotted in Fig. 11 for three

of the propagation directions. It is believed that the larger values of k correspond to the dimensions of the second zone, while the smaller values correspond to those of the third zone. The latter, however, are not very precise and so there is some doubt as to the correctness of their origin.

The curve of Fig. 11(a) corresponds to a quadrant of the central section shown in Fig. 2. In general features, the correspondence between the two is quite gratifying, particularly as regards the difference between the zone faces parallel and perpendicular to the c axis.[16] As would be expected, the sharp corners of the theoretical curve are rounded off in actuality and the contours of the zone faces are somewhat modified. Similar modifications are found in the curves of Figs. 11(b) and 11(c). The latter corresponds to the central cross section shown in Fig. 3 and clearly demonstrates that the (110) zone edges are not cusp-like. Figure 11(b) corresponds to a central section of the second zone taken perpendicular to [001] and again shows the remarkable accuracy with

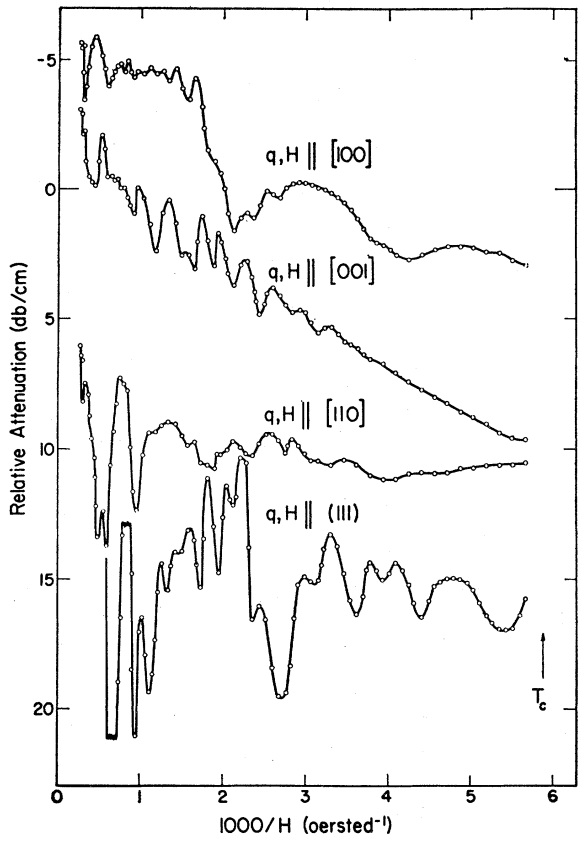

FIG. 9. Relative attenuation of 91-Mc/sec longitudinal waves propagating along various crystal directions as a function of a longitudinal magnetic field. The curves are displaced for clarity.

TABLE I. Comparison of theoretical and experimental dimensions of 2nd and 3rd zones in indium.[a]

Zone	Dimension designation	Theoretical dimension	Experimental dimension	Mean experimental
2	a	1.04	1.00 (1)[b]	0.99
			0.98 (3)	
	b	1.24	1.13 (2)	1.13
	c	1.13	0.97 (2)	1.00
			1.03 (3)	
	d	0.69	0.84 (4)	0.84
	e	0.69	0.89 (4)	0.89
3	f	0.42	0.47 (2)	0.47
	g	0.42	0.49 (4)	0.49
	h	0.30	0.35 (4)	0.35
	j	0.28	0.21 (1)	0.21

[a] All in units of 10^8 cm^{-1}.
[b] Crystals with $q\|(100)$, (001), (110), and (111) designated 1, 2, 3, and 4, respectively.

which the free-electron model predicts the shape of the second-zone surface. In all cases, however, the theoretical model overestimates the actual magnitude of the Fermi surface dimension by about 10%. The discrepancies for certain directions in k space are summarized in Table I, which gives both the theoretical and experimental dimensions. Such discrepancies are, of course, to be expected and have previously been observed in the extremal cross sections of lead obtained from dHvA measurements.[17] It is of interest that the dimensions d, e, of the second zone agree very well with those to be expected from the experimentally determined cross sections, even though they are much larger than the values predicted from the free-electron model.

No data obtained in his work have revealed any oscillations corresponding to the non-central orbits proposed by Roberts[18] to explain his measurements of the magnetoacoustic effect in aluminum. Contrary also to the situation in aluminum, it would appear that the scattering across the "square" faces of the second zone is not abnormally large for indium, since otherwise central orbits would not easily be observable. It would seem that further work is necessary to clarify the reason for the apparently different electron scattering in these two metals.

The situation with respect to the dimensions of the third zone is not very satisfactory. For certain directions of propagation, most notably $q\|[110]$, no oscillations corresponding to the third zone have been detected; the most pronounced effects seem to occur for $q\|(111)$. Reference to Table I shows that there seems to be reasonable agreement between theory and experiment for the "normal" cross sections of the arms α, β. This agreement must be accepted with caution, however, owing to the large uncertainties in the experimental data. It is somewhat disconcerting that in Fig. 11(b), the third-zone momentum *decreases* away from the

[16] *Note added in proof.* It should be noted that, in general, there is not an exact correspondence between the extremal dimensions obtained from the magnetoacoustic data and the actual diameters of the Fermi surface. This point is discussed fully in the paper of Gurevitch.

[17] A. V. Gold, Phil. Trans. Roy. Soc. (London) **A251**, 85 (1958).
[18] B. W. Roberts, Phys. Rev. **119**, 1889 (1960).

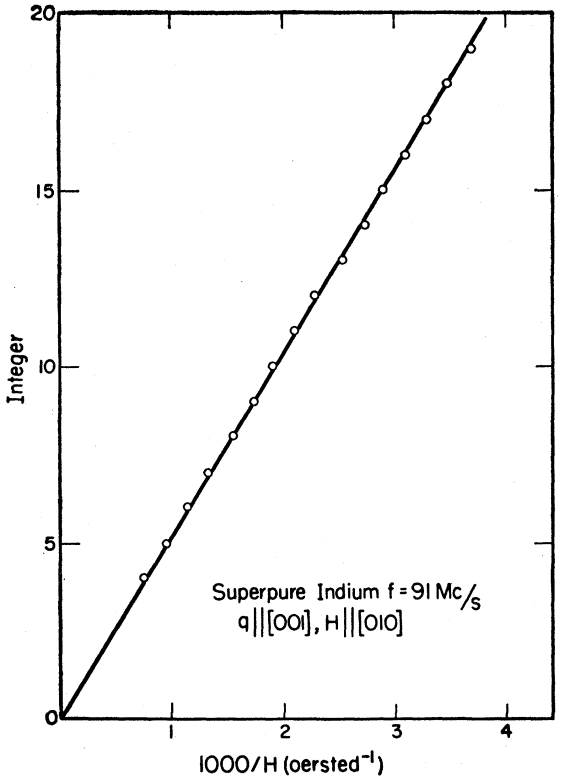

FIG. 10. Plot of integer versus attenuation maxima in $1/H$ for longitudinal wave propagating along [001] with a magnetic field along [010].

[110] direction. Such a decrease must imply that the arms are pinched away rather sharply from this direction. Even more puzzling is the large difference in the third-zone dimensions along the [001] and [010] directions observed in Fig. 11(b). Such behavior is not consistent with the shape of the arms derived from the free-electron model. It would thus appear that further measurements at much higher frequencies are desirable to obtain more accurate data for these dimensions.

Comparison with the work of Galkin *et al.*[8] is somewhat difficult because of the scatter in their data. It would appear, however, that the momenta corresponding to their principal oscillations are considerably smaller than those found in the present work. No explanation of this difference can be advanced. Contrary to what was found in the present experiments, their data gives the most accurate third-zone momenta for $q\|[\bar{1}10]$. In particular, for $H\|[110]$, they obtain $\Delta(1/H)=6.8\times10^{-4}$ oersted^{-1}; $k_{\text{ext}}=0.30\times10^{8}$ cm^{-1} as compared to the value of 0.47×10^{8} cm^{-1} found here. As noted previously, resolution of these discrepancies will have to await more accurate high-frequency data on third-zone dimensions. No oscillations corresponding to momenta larger than the zone dimensions were observed in the present work, again in contrast to the findings of Galkin *et al.*

Figure 9 shows the results of magnetoacoustic measurements with $\mathbf{q}\|\mathbf{H}$. It can be seen that oscillatory behavior is also present for this geometry, but that the oscillations do not appear to be periodic in $1/H$. There does not appear to be any theoretical treatment for this case and no simple explanation of the effect can be advanced.

(b) High-Field Attenuation

Reference to Figs. 5–8 shows that, superimposed in the oscillatory behavior, there appears to be a large increase in the attenuation for increasing magnetic field, H. In all cases studied, the attenuation reached a saturation value, thereby confirming the nonexistence of open orbits at least in these directions. The saturation values of attenuation relative to the zero-field values for $q\|[001]$ and $q\|[100]$ are given in Figs. 12 and 13 as a function of the direction of the magnetic field. It will be seen that, except for $q\|[001]$, $H\|[100]$, the saturation attenuation exceeds the zero-field value. This result is in agreement with the conclusions of Kjeldaas and Holstein[9] who find that the zero-field attenuation is greater than or less than the saturation value according as ql is less than or greater than $5\pi/2$. In the experiments $ql>400$, so that the latter condition is amply fulfilled.

Pippard has considered the high-field limit of attenuation for a nonspherical Fermi surface. For this case of interest here, he finds that for closed orbits

$$\lim_{H\to\infty}\alpha_{ik}=(\hbar^2q^2/2\pi^2Mv_s)\int(\bar{\tau}/m_c)I_0^2dk_z, \quad (5)$$

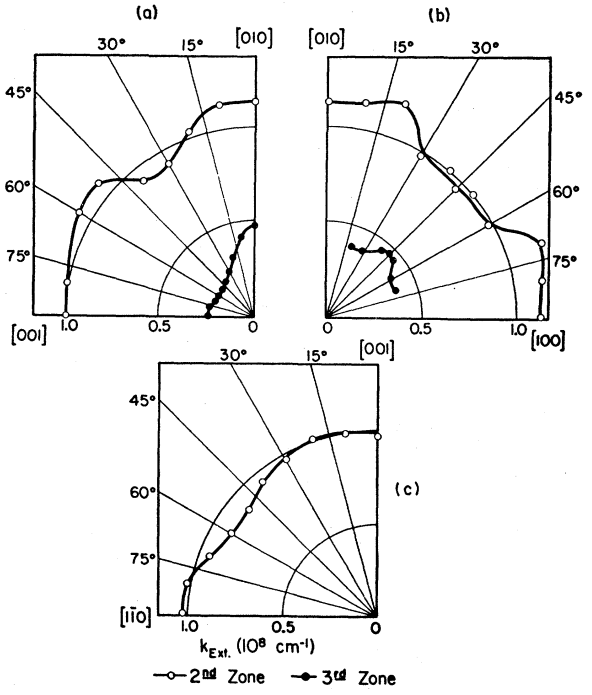

FIG. 11. Extremal dimensions of second and third zones of indium obtained from magnetoacoustic data. The second-zone dimensions are extremal radii, while the third-zone dimensions are extremal diameters.

where M is the density of the material, v_s the sound velocity for the propagation direction i, m_c the cyclotron mass for the field direction, and τ the relaxation time. The integral also contains I_0, which itself is an integral involving the deformation parameter. Clearly since the Fermi surface is nonspherical and τ is presumably anisotropic, α_{ik} would also be anisotropic. Because of the complexity of the Eq. (5), however, it would be difficult to draw any conclusions regarding the variation of τ from the observed anisotropy in attenuation.

V. CONCLUSIONS

From these experiments it is concluded that the free-electron model gives a surprising accurate picture of the Fermi surface of indium. The experimental second-zone dimensions are some 10% smaller than those predicted theoretically. While the agreement between theory and experiment is somewhat less satisfactory for the third-zone dimensions, it is believed that the discrepancy is due at least in part to the rather poor accuracy of the experimental data. Further work is thus necessary to clear up this situation.

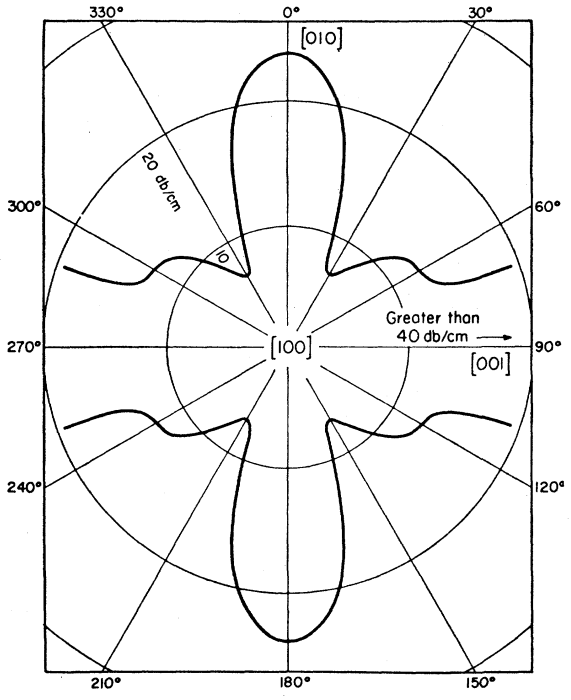

FIG. 12. Saturation values of attenuation ($H\sim20$ kgauss) for longitudinal waves propagating along [100] as a function of the direction of applied transverse field. The attenuation is measured relative to zero-field value for $q\|[100]$.

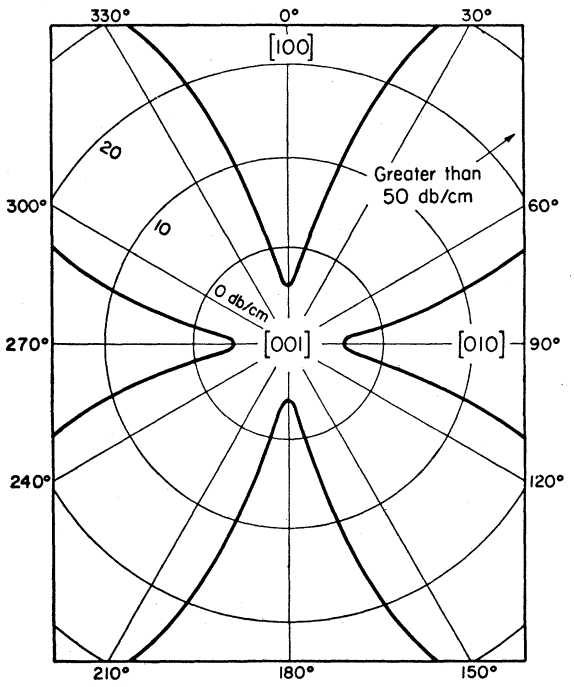

FIG. 13. Saturation values of attenuation ($H\sim20$ kgauss) for longitudinal waves propagating along [001] as a function of the direction of applied transverse field. The attenuation is measured relative to zero-field value for $q\|[001]$.

ACKNOWLEDGMENTS

Thanks are due to Dr. W. A. Harrison for several helpful discussions and to Dr. A. Mackintosh who independently supplied the authors with drawings of the central sections of the second and third zones in indium.